ERK-dependent mTOR pathway is involved in berberine-induced autophagy in hepatic steatosis

Qin He[1], Dan Mei[1], Sha Sha[1], Shanshan Fan[1], Lin Wang[2] and Ming Dong[1]

[1]Department of Endocrine and Metabolism, Qilu Hospital of Shandong University, Shandong University, Ji'nan, Shandong, China
[2]Department of Endocrine and Metabolism, Jiaxiang People's Hospital, Ji'ning, Shandong, China

Correspondence should be addressed to M Dong
Email
dr_dongming@126.com

Abstract

Non-alcoholic fatty liver disease (NAFLD) is a burgeoning health problem and is considered as a hepatic manifestation of metabolic syndrome. Increasing evidence demonstrates that berberine (BBR), a natural plant alkaloid, is beneficial for obesity-associated NAFLD. However, the mechanisms about how BBR improves hepatic steatosis remain uncertain. Recently, some reports revealed that enhanced autophagy could decrease hepatic lipid accumulation. In this study, we first established a high-fed diet (HFD) mice model and oleate–palmitate-induced lipotoxicity hepatocytes to explore the association among BBR, autophagy and hepatic steatosis. Our data demonstrated that BBR had profound effects on improving hepatic lipid accumulation both *in vivo* and *in vitro*, and led to high autophagy flux. The molecular alterations proceeding these changes were characterized by inhibition of the ERK/mTOR pathway. These findings suggest an important mechanism for the positive effects of BBR on hepatic steatosis, and may provide new evidence for the clinical use of BBR in NAFLD.

Key Words
- berberine
- hepatic steatosis
- autophagy
- ERK
- mTOR

Journal of Molecular Endocrinology
(2016) **57**, 251–260

Introduction

Non-alcoholic fatty liver disease (NAFLD) is known as a common liver disease in adults and children, which refers to a wide spectrum of liver damage from steatosis to non-alcoholic steatohepatitis, and cirrhosis ultimately. It is also a risk factor for metabolic diseases, including type 2 diabetes, obesity and dyslipidaemia (Tiniakos *et al.* 2010). Thus, NAFLD is often considered as the hepatic manifestation of metabolic syndrome. To date, no effective medical interventions exist that could completely reverse NAFLD other than lifestyle changes, dietary alterations and, possibly, bariatric surgery. Therefore, it is reasonable to explore new therapeutic strategies for this disease.

Berberine ($C_{20}H_{19}NO_5$, BBR), an isoquinoline alkaloid isolated from *Berberis vulgaris* L, has been widely used in traditional Chinese medicine to treat diarrhoea, insulin resistance, inflammation and gastrointestinal disorders. Recently, there is fast-growing concerns in exploring its activities in neurons and metabolism (Lu *et al.* 2015). Of interest, BBR also displays an important role in hepatic disease as supported by the studies from both animal and clinical researches (Kim *et al.* 2009, Yan *et al.* 2015). However, specific mechanisms that underlie the improvement of hepatic steatosis by BBR are poorly delineated.

Autophagy is a cellular process otherwise known as programmed cell death type 2, which may lead to a form of non-apoptotic cell death (Park *et al.* 2007, Pyo *et al.* 2005), sequestering senescent, dysfunction

http://jme.endocrinology-journals.org
DOI: 10.1530/JME-16-0139

Published by Bioscientifica Ltd.

or damaged organelles/proteins in autophagosomes for recycling of their products (Levine & Kroemer 2008). Moreover, autophagy is also involved in eliminating cells that have passed through classical type 1 programmed cell apoptosis or death. Under physiological conditions, autophagy takes part in the basal turnover of lipids by engulfing and decreasing lipid droplets (Lavallard & Gual 2014). Important links between the regulation of autophagy, obesity and liver complications have been reported (Jung *et al.* 2015). In addition, some studies have demonstrated that BBR could be used to improve hepatic steatosis (Guo *et al.* 2016), and others have also revealed that BBR could induce autophagy in liver cancer cells (Wang *et al.* 2010). However, the exact mechanisms about its effects and potential autophagy pathways in hepatic steatosis remain to be elucidated.

The mammalian target of rapamycin (mTOR) pathway has been demonstrated to play a significant role in controlling many critical cellular processes, such as cell growth, protein synthesis and transcription (Le *et al.* 2016). Recent studies have shown that mTOR is involved in lipid metabolism (Han *et al.* 2016). An essential feature of this signalling cascade is protein activation by multisite phosphorylation. Extracellular signal-regulated kinase (ERK) is one of the upstream targets of mTOR and negatively regulates mTOR, hence enhancing autophagy flux (Li *et al.* 2016). ERK, one of mitogen-activated protein kinase (MAPK) cascades, is also a central integrator of various extracellular signals ranging from single distinct cytokines or hormones to cellular mechanical stress that influences lipid metabolism and other cellular changes (Knebel *et al.* 2014). Some studies have revealed that BBR have effects on THP-1 cells by targeting MAPK pathway (Gao *et al.* 2014). However, the potential role and underlying mechanisms of ERK/mTOR pathway in mediating BBR-induced autophagy in hepatocytes remain largely unknown.

This study ought to explore the mechanisms of the effects of BBR on hepatic steatosis and the potential signalling pathway. We set up an obesity mouse model with a high-fat diet (HFD) and induced hepatocyte steatosis with free fatty acids (FFA) in human L-O2 cells. BBR and two inhibitors of autophagy, chloroquine (CQ) and bafilomycin A1 (Baf), were added into each group, respectively. We first explored the effects of BBR on liver fat and intracellular lipids, and then autophagy-related proteins were determined, including microtubule-associated protein 1 light chain 3 (LC3) and SQSTM1 (p62). Finally, ERK/mTOR signalling pathway was observed in order to reveal the potential molecular pathway underlying the autophagy-promoting role of BBR.

Materials and methods

Reagents

Berberine chloride (BBR), bafilomycin A1 (Baf), chloroquine (CQ) and dimethyl sulphoxide (DMSO) were obtained from Sigma-Aldrich (PHR1502, B1793, C6628, D2650). Rabbit anti-LC3B, SQSTM1 (p62), Beclin-1, mTOR/p-mTOR (Ser2448), 70S6K/p-70S6K (Thr389), 4E-BP1/p-4E-BP1 (Ser65), ERK/p-ERK (Thr202/204) and GAPDH antibodies were purchased from Cell Signaling Technology.

Animal study

Fifty six-week-old male C57BL/6 mice (obtained from the Model Animal Research Center of Shandong University, Jinan, China) were used for the experiments. Ten wild-type (WT) mice were fed with regular mouse chow (WT + chow), and the rest 40 mice with HFD (WT + HFD). The HFD (D12492, New Brunswick, NJ, USA) contained 60 kcal% fat, whereas the regular mouse chow contained 11 kcal% fat. Body weight (BW), food intake and glucose from the caudal vein was monitored weekly.

After 12 weeks, the HFD-fed mice were divided into the following groups: WT + HFD ($n=10$), HFD + BBR ($n=10$), HFD+CQ ($n=10$) and HFD + CQ + BBR ($n=10$). Control mice (WT + HFD) received intra-peritoneal injection of saline, whereas treated mice received BBR (50 mg/kg/day), CQ (25 mg/kg/day) and BBR (50 mg/kg/day) plus CQ (25 mg/kg/day) once daily for another 6 weeks. IPGTT and IPITT were performed after 4 weeks of BBR administration. Meanwhile, BW, food intake and glucose from the caudal vein were monitored weekly.

Cell culture

L-O2 cells (obtained from China Cell Culture Center, Shanghai, China), the human hepatic cell line, were cultured in Dulbecco's modified Eagle's medium (DMEM, SH30022.01B, Hyclone, UT, USA) with 10% foetal bovine serum (10082147, Gibco), penicillin (100 UI/mL) and streptomycin (100 UI/mL). All cell cultures were maintained in a 37°C incubator with 5% CO_2.

Journal of Molecular Endocrinology

http://jme.endocrinology-journals.org
DOI: 10.1530/JME-16-0139

Published by Bioscientifica Ltd.

To induce steatosis, L-O2 cells were exposed to 1 mmol/L FFAs (oleate and palmitate, 2:1; Sigma-Aldrich) mixture for 24 h, whereas the control cells were incubated in the normal medium. To investigate the role of autophagy in the treatment of hepatic steatosis by BBR, the FFA-induced hepatocytes then divided into the following groups: FFA, FFA + BBR (0.2 μM, 1 μM, 5 μM), FFA + Baf and FFA + Baf + BBR. BBR and Baf (30 nM; B1793, Sigma-Aldrich) were added into the above-indicated cell cultures and cultured for another 24 h. Finally, SCH772984 (SCH, 1 μM, S7101, Selleck), the ERK inhibitor, was added to explore the potential signalling pathway.

Immunohistochemistry

Slides with paraffin sections were deparaffined and rehydrated. For antigen retrieval, slides were boiled in a 10 mM citrate buffer (pH 6.0) for 10 min. The slides were incubated with primary antibody of anti-LC3 overnight at 4°C, followed by incubation with the secondary antibody of goat anti-rabbit and DAB as chromogen. The images were then obtained using an optical microscope.

Haematoxylin and eosin staining

All tissue samples were treated with standard haematoxylin and eosin staining techniques, after which these samples were evaluated for pathological changes by an optical microscope.

Oil red O staining

After BBR treatment, cells were fixed with 4% paraformaldehyde for 15 min, then stained with oil red O (for preparation, put 0.5 g into 100 mL isopropanol, then remove 6 mL and then add 4 mL distilled water) for 15 min. Cells were treated with 60% isopropanol and dyed with haematoxylin, then rinsed with PBS three times before microscopic examination.

Immunofluorescence microscopy

Cells were incubated with anti-LC3 antibody, followed by the incubation with corresponding fluorescence-conjugated secondary antibody for 1 h at room temperature. Subsequently, cell nuclei were stained with DAPI (Boyetime Institute of Biotechnology, Shanghai, China) for 5 min away from light. Finally, images were obtained using an Olympus BX61 fluorescence microscope.

Liver tissue and intracellular lipid profiles test

Total cholesterol and triglyceride levels within liver tissues and L-O2 cells were determined by an automatic biochemistry analyzer (COBAS80000, c702, Swit). First, tissues or cells were washed twice with PBS and cell lysis buffer was added (5% NP-40), then they were collected into centrifuge tubes and heated at 70°C for 10 min. Finally, after being centrifuged at 2000 × *g* for 5 min, supernatants were collected for lipid profiles measurement.

Transmission electron microscopy

Liver tissues and L-O2 cells were fixed with 2.5% glutaraldehyde and post-fixed with 1% osmium tetroxide at 4°C. The samples were then dehydrated through a graded series of ethanol concentrations (15 min each). After being embedded with 100% acetone and embedding solution, the specimens were sliced into semi-thin sections (50 nm), which were then stained with uranyl acetate and lead citrate. Images were captured with a transmission electron microscope (EM902A, Carl Zeiss MicroImaging GmbH, Germany).

Western blot analysis

Liver tissues and L-O2 cells were subjected to Western blot analysis, according to standard protocols. Membranes were incubated with appropriate primary and secondary antibodies, proteins were visualized using Millipore's enhanced chemiluminescence and analyzed with the Quantity One software (BioRad).

Statistical analysis

Three independent experiments were performed, and the data were expressed as the mean ± S.E.M. from multiple samples. GraphPad Prism 5 software was used for statistical analyses. Data were analyzed using paired *t*-test, $P < 0.05$ was regarded as statistically significant (*$P < 0.05$; **$P < 0.01$).

Results

BBR reduces BW, improves glucose tolerance and promotes insulin sensitivity in HFD-fed mice

The BW and food intake (kcal/kg/h) of mice fed with HFD were both significantly increased than those in chow-fed group from 4 to 12 weeks (Fig. 1A and B). After BBR treatment, the BW showed significant decrease in

http://jme.endocrinology-journals.org
DOI: 10.1530/JME-16-0139

Published by Bioscientifica Ltd.

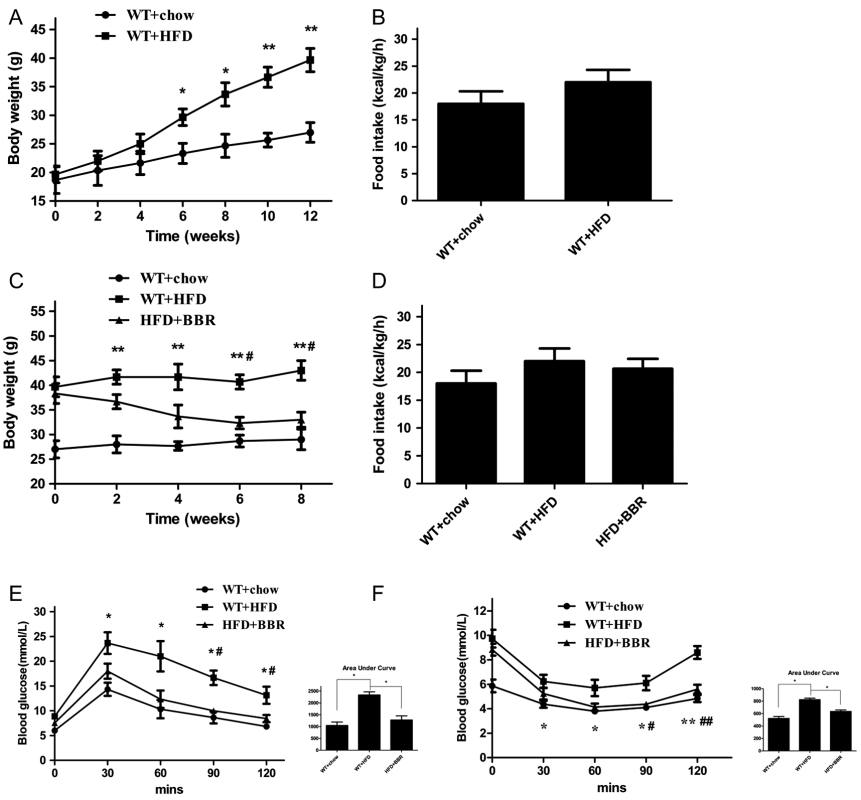

Figure 1
Effects of BBR on BW and glucose homeostasis in C57BL/6 mice. (A) Body weight (BW) was measured every 2 weeks during HFD-fed. (B) Average food intake was calculated based on food consumption during HFD-fed before BBR treatment. (C) BW during BBR treatment and detected every 2 weeks. (D) Average food intake during BBR treatment. (E) IPGTT after BBR treatment and area under the curve. (F) IPITT after BBR treatment and area under the curve. For A, C, E and F, $^{*}P<0.05$; $^{**}P<0.01$ WT + chow vs WT + HFD; $^{\#}P<0.05$; $^{\#\#}P<0.01$ WT + HFD vs HFD + BBR. Data are expressed as mean ± S.E.M. (n= 10).

HFD-fed mice (Fig. 1C), while the food intake inhibition was not evident (Fig. 1D). The fasting blood glucose level of HFD-fed mice was higher than that of chow-fed mice, and showed a significant reduction after BBR treatment (Fig. 1E). The results of IPGTT and IPITT are shown in Fig. 1E and F, which revealed that BBR could reduce blood glucose levels and improve insulin sensitivity in HFD-fed mice.

BBR improves liver weight and serum lipid profile in HFD-fed mice

We collected and weighed the livers, and detected the serum lipid profiles after all treatments. As expected, the liver weight in HFD-fed mice was dramatically decreased after BBR treatment (Table 1). The serum lipids profile, including total cholesterol, triglyceride, high-density lipoprotein cholesterol (HDL-C) and low-density lipoprotein cholesterol (LDL-C) were tested in this study. We found that above indexes were maintained or even improved dramatically in BBR-treated HFD mice (Table 1).

BBR-induced autophagy reduces hepatic lipid accumulation in HFD-fed mice

Photographs showed the livers exhibited bigger size irrespective of BBR treatment in HFD-fed mice (Fig. 2A). Haematoxylin and eosin staining revealed a significant

Table 1 BBR improved liver weight and lipid profile in C57BL/6 mice.

	WT + chow	WT + HFD	HFD + BBR
Liver weight (g)	0.928–0.08	1.788–0.173*	1.137–0.128
Serum			
Cholesterol (mmol/L)	2.482–0.23	4.822–0.387*	2.894–0.286#
Triglyceride (mmol/L)	0.564–0.05	1.02–0.777*	0.704–0.057#
HDL (mmol/L)	1.96–0.26	3.589–0.329*	2.559–0.286
LDL (mmol/L)	0.293–0.05	0.553–0.11	0.367–0.04

After 12 weeks of HFD induction and 6 weeks of BBR treatment, mice were fasted overnight and anesthetized with chloral hydrate before being killed. Blood was collected to measure the levels of lipid (TG, TC, HDL, LDL), and livers were collected and weighed. $^{*}P<0.05$ vs WT + chow; $^{\#}P<0.05$ vs WT + HFD. Data are expressed as mean ± S.E.M. (n = 10).

http://jme.endocrinology-journals.org
DOI: 10.1530/JME-16-0139

Published by Bioscientifica Ltd.

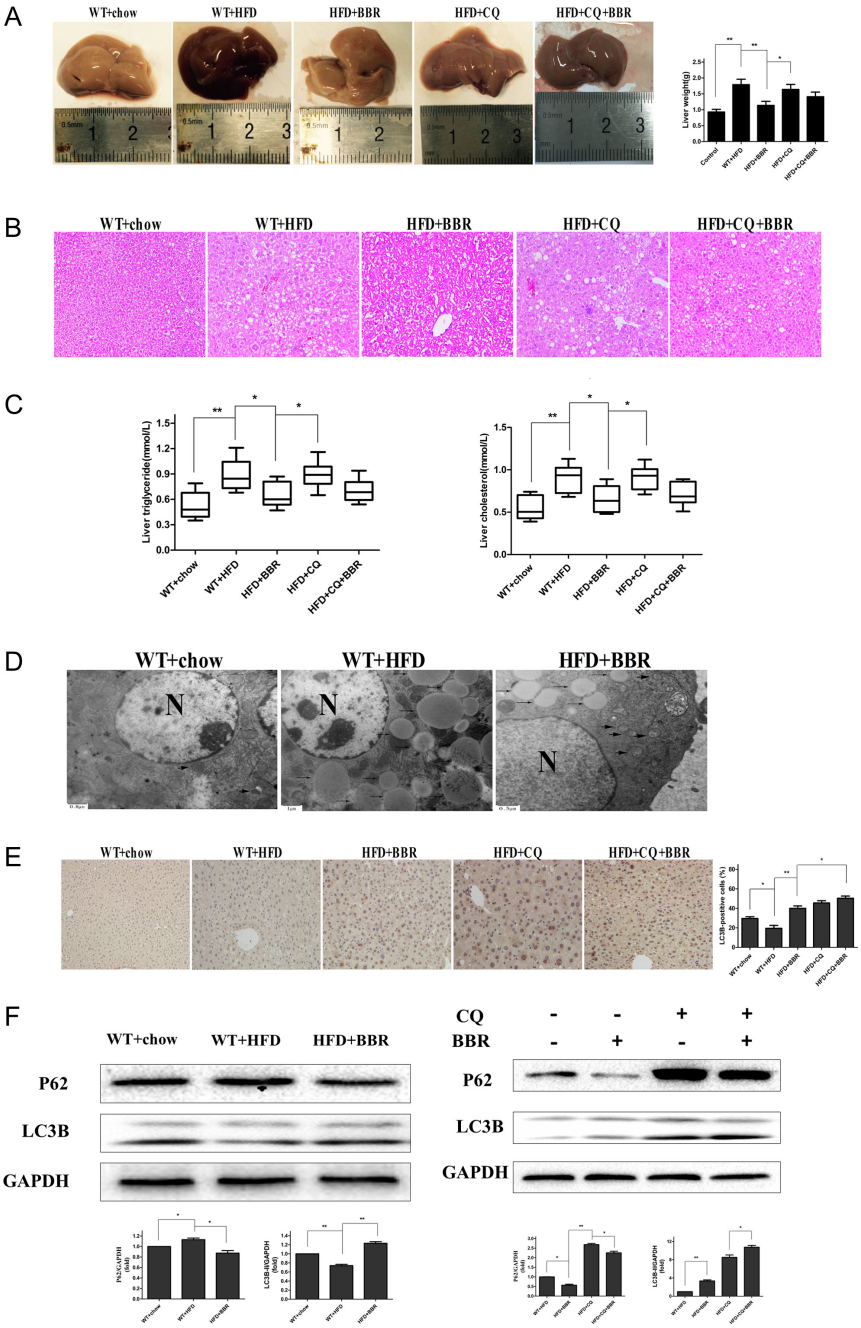

Figure 2
BBR-induced autophagy reduces hepatic lipid accumulation in HFD-fed mice. (A) General photographs showed liver size. (B) Liver sections with H&E staining. Photomicrographs were taken by a microscope with original magnification 20×. (C) Liver triglyceride and cholesterol were measured. (D) Images from transmission electron microscopy (TEM) of livers; coarse arrows, characteristic autophagosomes; thin arrows, lipid droplets; *N*, nucleus. (E) Immunohistochemical staining results of LC3B on liver sections with BBR (50 mg/kg/day) treatment in the absence or presence of CQ. The charts indicate the percentage of LC3B-positive cells. (F) Western blot analyses for LC3B-II and P62 in livers after BBR treatment in the absence or presence of CQ. GAPDH served as the loading control. The relative LC3B-II/GAPDH and p62/GAPDH ratios were calculated using ImageJ 1.36b. All data are expressed as mean ± S.E.M. ($n = 10$). $^{*}P < 0.05$; $^{**}P < 0.01$.

increase of lipid droplets in hepatocytes of HFD-fed mice compared with chow-fed group, but dramatically decreased after BBR treatment (Fig. 2B). Consistently, TG and TC contents in the livers were reduced in HFD-fed mice with BBR treatment compared with the saline group, respectively (Fig. 2C). CQ, the autophagy inhibitor, could narrow the effects induced by BBR (Fig. 2A, B and C). Transmission electron microscopy is well recognized as the golden standard to observe autophagosomes. It revealed scarce autophagosomes in chow-fed control mice, while abundant characteristic autophagosomes in hepatocytes treated with BBR (Fig. 2D). LC3 is required for the formation of autophagosome, increasing accumulation of LC3 light chain puncta and LC3B-II conversion always indicate the activation of autophagy. Due to interaction with LC3B, p62 is constantly degraded via autophagy and autophagy inhibition results in the accumulation of p62 positive aggregates (Zhang *et al.* 2016*a*). Immunohistochemistry revealed significantly unregulated LC3B level in BBR-treated HFD-fed mice (Fig. 2E). Furthermore, a combination of BBR

http://jme.endocrinology-journals.org
DOI: 10.1530/JME-16-0139

Published by Bioscientifica Ltd.

and CQ treatment resulted in a massive LC3B accumulation (Fig. 2E). As shown in Western blot, the level of LC3B-II was more pronounced with an increased dose of BBR in HFD-fed mice, whereas P62 was less expressed (Fig. 2F). To test whether BBR-induced upregulation of LC3B and downregulation of P62 are due to autophagy induction, CQ, which prevents the late stage of autophagy by inhibiting lysosomal protein degradation (Liu *et al.* 2016), was used to inhibit autophagic flux. Although increased levels of LC3B-II and P62 were detected in CQ-treated group, LC3B-II was even higher and P62 decreased slightly when co-used with BBR and CQ, indicating that BBR induces autophagy in HFD-fed mice (Fig. 2F).

BBR-induced autophagy reduces hepatic lipid accumulation in steatotic L-O2 cells

As shown in Fig. 3, oil red O staining of FFA-induced L-O2 cells clearly confirmed that intracellular lipid accumulation was significantly decreased after BBR treatment, and also

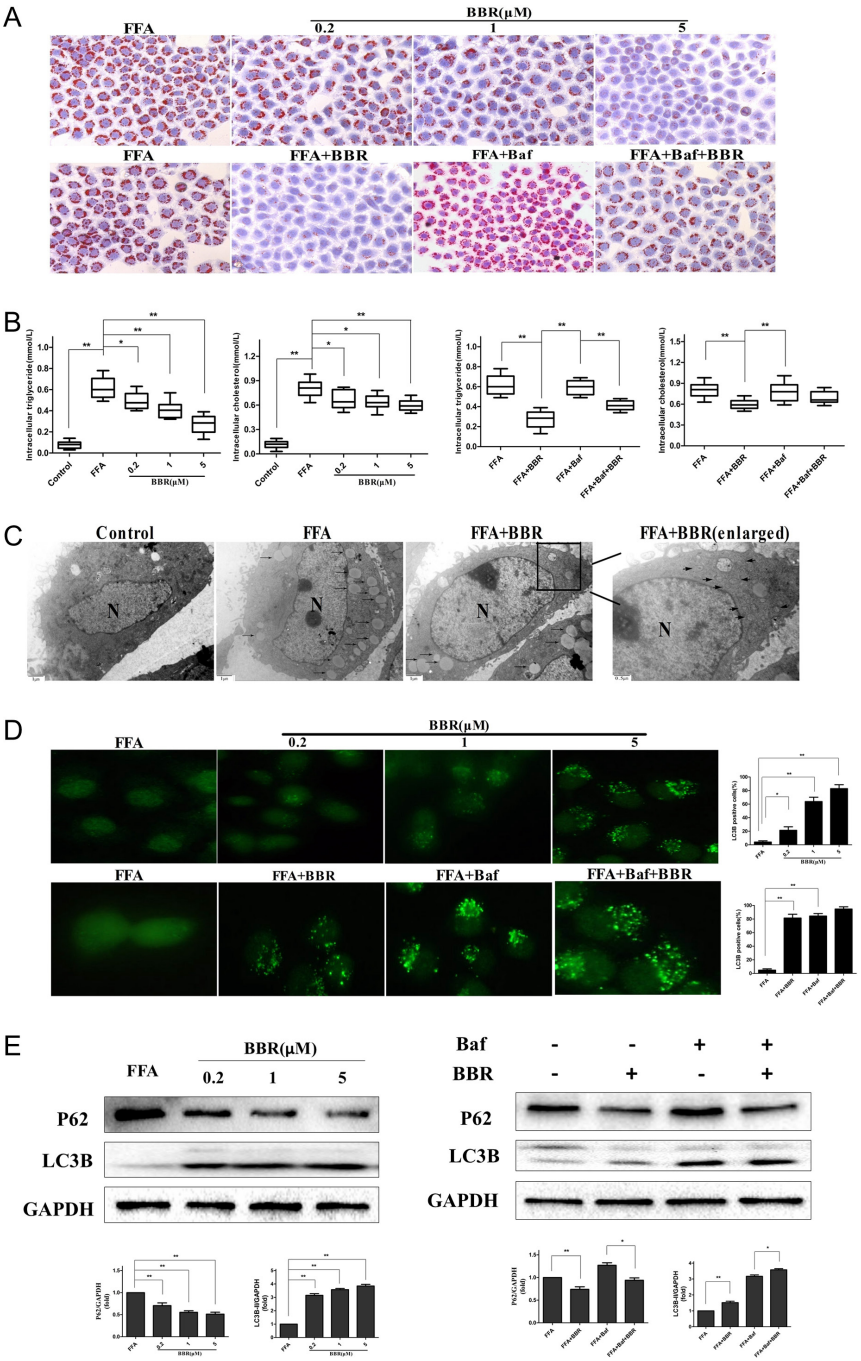

Figure 3
BBR-induced autophagy reduces hepatic lipid accumulation in steatotic L-O2 cells. (A) Oil red O staining of hepatocytes after BBR-treated 24 h. (B) Intracellular triglyceride and cholesterol were quantified. (C) Transmission electron microscopy (TEM) of L-O2 cells in the groups given various treatments; coarse arrows, characteristic autophagosomes; thin arrows, lipid droplets; *N*, nucleus. (D) Immunofluorescence staining results of LC3B on L-O2 cells with BBR (0, 0.2 μM, 1 μM, 5 μM) and Baf (30 nM) treated for 24 h. (E) LC3B-II and p62 levels were examined by Western blot analysis for hepatocytes after BBR treatment in the absence or presence of Baf (30 nM). GAPDH served as the loading control. The relative LC3B-II/GAPDH and p62/GAPDH ratios were calculated using ImageJ 1.36b. All data are expressed as mean ± S.E.M. $*P<0.05$; $**P<0.01$.

Journal of Molecular Endocrinology

http://jme.endocrinology-journals.org
DOI: 10.1530/JME-16-0139

Published by Bioscientifica Ltd.

dose-dependently (Fig. 3A). Lipid profiles test revealed that TC and TG levels increased obviously in FFA-induced L-O2 cells compared with control group, and dramatically reduced after BBR treatment in a dose-dependent manner (Fig. 3B). However, a combination of BBR and Baf resulted in intermediate effects in steatolysis (Fig. 3A and B). Numerous mitochondria and few autophagosomes were observed in control L-O2 cells, whereas a large amount of autophagosomes and less lipid droplets were present in steatotic L-O2 cells after BBR treatment (Fig. 3C). Immunofluorescence staining showed that the LC3B expression level was upregulated in the FFA-induced L-O2 cells treated with BBR in a dose-dependent manner, which was even higher when used together with Baf (Fig. 3D). Autophagy-associated proteins, LC3B-II and p62, were examined by Western blot. The results showed that the level of LC3B-II was increased while that of p62 was decreased when treated by BBR, also dose-dependently (Fig. 3E), indicating an enhancement of autophagic flux. Baf, which prevents the late phase of autophagic flux by inhibiting the fusion of autophagosomes with lysosomes (Liu *et al.* 2016), gave results similar to CQ, enhanced both p62 and LC3B-II levels, so that a combination of BBR and Baf resulted in higher LC3B-II and intermediate P62 level (Fig. 3E).

ERK/mTOR signalling pathway is involved in BBR-induced autophagy in L-O2 cells

mTOR acts as a central regulator in autophagy induction, and ERK modulates the activation of mTOR (Li *et al.* 2016).

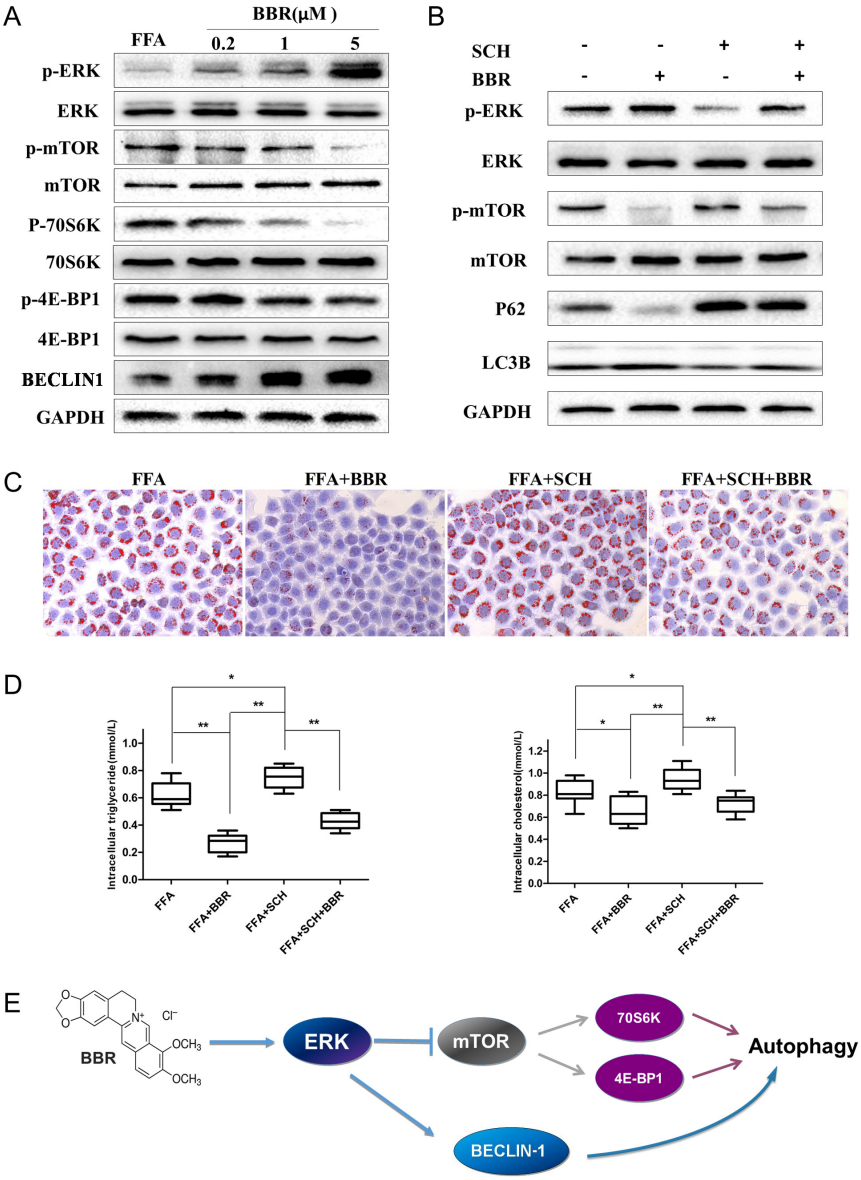

Figure 4
ERK/mTOR signalling pathway is involved in BBR-induced autophagy in hepatocytes. Western blot analysis of p-ERK, ERK, p-mTOR, mTOR, 70S6K/p-70S6K, 4E-BP1/p-4E-BP1, Beclin-1 and GAPDH expression in hepatic L-O2 cells (A) treated with BBR. (B) Western blot analysis of p-ERK, ERK, p-mTOR, mTOR, p62, LC3B-II and GAPDH treated with BBR in the absence or presence of SCH (1 μM) in L-O2 cells. (C) Oil red O staining of L-O2 cells after BBR treatment in the absence or presence of SCH. (D) Intracellular triglyceride and cholesterol were quantified in L-O2 cells. (E) A schematic diagram of autophagy induced by BBR in hepatocytes. All data are expressed as mean ± S.E.M. $^{*}P<0.05$; $^{**}P<0.01$.

Journal of Molecular Endocrinology

http://jme.endocrinology-journals.org
DOI: 10.1530/JME-16-0139

Published by Bioscientifica Ltd.

We, therefore, detected the levels of p-ERK, p-mTOR as well as mTORC1 substrates p-70S6K and p-4E-BP1 in L-O2 cells. As shown in Fig. 4A, levels of p-mTOR, p-70S6K (Thr389) and p-4E-BP1 (Ser65) were downregulated while p-ERK was upregulated when treated with BBR for 24 h and in a dose-dependent manner. Beclin-1, a regulator of autophagy, was increased simultaneously (Fig. 4A). It indicated that the ERK-modulated mTOR pathway might be involved when autophagy occurred after BBR treatment. In addition, activation of the pathway was partially restored when cells were treated simultaneously with a novel ERK inhibitor, SCH, which could dephosphorylate ERK and increase phosphorylation of mTOR in BBR-treated cells, hence inhibiting BBR-induced autophagy flux (Fig. 4B). Subsequently, oil red O staining and intracellular lipid profiles were detected to further explore the role of ERK in FFA-induced L-O2 cells. The data revealed that intracellular lipid accumulation, TC and TG levels, increased slightly in SCH-treated group compared with the results when FFA used alone, and then decreased significantly when co-used with BBR (Fig. 4C and D). Thus, it further established ERK-mediated mTOR signalling as a molecular signalling for BBR improvement of hepatic steatosis. Figure 4E shows a schematic diagram of autophagy induced by BBR in hepatocytes.

Discussion

The incidence of NAFLD ranges from 20% to 30% worldwide, and is currently considered as a hepatic manifestation of metabolic syndrome, which is associated with the increased risk of cardiovascular disease and mortality in the general population. Moreover, NAFLD ranging from simple lipid accumulation to non-alcoholic steatohepatitis is becoming one of the most common aetiologies of liver fibrosis, which may eventually cause hepatic carcinoma. Novel therapeutic strategies that efficaciously target lipid metabolism are needed desperately to improve the currently unfavourable outcome of patients with NAFLD. Some studies have provided compelling evidence that BBR could reduce BW and improve metabolic syndrome (Zhang *et al.* 2012). Furthermore, BBR reduces insulin resistance by upregulation of IRS-2 mRNA expression and improves insulin sensitivity by upregulation of IRS-1 tyrosine phosphorylation (Liu *et al.* 2010). However, the mechanistic basis for these effects is poorly reported in hepatocytes. In this study, we demonstrated that BBR significantly decreased liver weight and had a profound effect on improving hepatic lipid accumulation both *in vivo* and *in vitro*. IPGTT and IPITT analysis showed that BBR significantly improved glucose tolerance and insulin sensitivity in the HFD-fed mice. Above results support the view that BBR could improve insulin sensitivity through decreasing BW and hepatic lipid content (Guo *et al.* 2016).

Autophagy is important in controlling cellular metabolism and energy homeostasis, and alterations of autophagy have been reported to be associated with the development of metabolic syndrome (Kim *et al.* 2013). Lipid metabolism plays a major role in modulating both energy storage and energy homeostasis. Small molecules that regulate autophagy in lipid metabolism could be valuable targets to indicate autophagy mechanisms and develop treatments for obesity-related NAFLD. Ma *et al.* found that deletion of FIP200, a core subunit of the mammalian autophagy-related 1 complex, could reduce HFD-induced steatosis and downregulated the gene expression of enzymes involved in *de novo* lipogenesis (Ma *et al.* 2013). Several reports have illustrated that BBR improved cell function by promoting autophagy. Zhang *et al.* found that BBR-induced autophagy and exerted protective effects on neuron *in vitro* and *in vivo* (Zhang *et al.* 2016*b*). As mentioned above, autophagy is deemed to be at least one of the critical mechanisms in regulating lipid metabolism; hence, we aimed in this study to explore the association between BBR and autophagy in hepatic steatosis. In this study, the increase of autophagosomes in BBR-treated hepatocytes was also confirmed by the elevated expression of LC3B-II, a marker of autophagy (Figs 2F and 3E). Further experiments were performed to demonstrate above results by using BBR together with CQ or Baf. The data revealed that BBR partially reverses the change in liver lipid content when autophagy is inhibited and this is supported by the cell data in Fig. 3, which indicated that the reduction of hepatic lipid droplets was associated with a concomitant increase in autophagy flux. It suggested that autophagy may play an absolutely necessary role in lipolysis, which could provide a new way to eliminate lipid accumulation in addition to lipase-mediated lipolysis.

Autophagy is regulated by a complex signalling network, most of which feed into the mTOR-dependent pathway (Wullschleger *et al.* 2006). A recent study relevant to the mechanisms of autophagy indicated that mTOR pathway was involved in the insulin resistance of pancreatic beta cells (Lakshmipathi *et al.* 2016),

http://jme.endocrinology-journals.org
DOI: 10.1530/JME-16-0139

Published by Bioscientifica Ltd.

but similar research in hepatocytes is rare. Our previous works have also indicated that GLP-1 agonist could improve hepatic lipid accumulation by inducing autophagy via AMPK/mTOR pathway. To reveal the potential mechanisms about the BBR-induced autophagy, the mTOR signal pathway was explored. Our results showed that BBR suppressed the levels of p-mTOR, p-70S6K and p-4E-BP1 in lipotoxicity hepatocytes (Fig. 4A), indicating that mTOR-dependent pathway may be involved in BBR-induced autophagy. As mentioned above, ERK is one of the upstream targets of mTOR and activates downstream signalling, results in enhancing autophagy flux (Knebel *et al*. 2014). In our *in vitro* study, ERK was activated and p-mTOR level was decreased in BBR-treated hepatocytes (Fig. 4A), which were, however, partially restored in the presence of SCH, a novel ERK inhibitor. As some reports demonstrated that BBR actions on ameliorating hepatic steatosis were probably attributable to BBR suppression of inflammation, improving insulin sensitivity and reducing endoplasmic reticulum stress (Guo *et al*. 2016, Xing *et al*. 2011, Zhang *et al*. 2016*c*), resulting in the effects induced by BBR could not completely prevent by ERK inhibitor. Therefore, the intracellular lipid accumulation was increased slightly after SCH treatment, and it could be partially reversed by BBR. Taken together, ERK-mediated mTOR signalling might provide a molecular basis of BBR-induced autophagy for improving hepatic steatosis. To the best of our knowledge, it is the first report about ERK-dependent mTOR pathway that was involved in BBR-induced autophagy in hepatocytes.

In summary, our data indicates that ERK-mediated mTOR signalling is critical for autophagy induced by BBR in hepatic steatosis. These findings suggest an important mechanism for the positive effects of BBR on hepatic steatosis, and may validate the potential use of BBR for the treatment or prevention of obesity-associated NAFLD.

Declaration of interest

The authors declare that there is no conflict of interest that could be perceived as prejudicing the impartiality of the research reported.

Funding

This work was supported by the Medical and Health Science & Technology development plan of Shandong Province (no. 2014WS0136), and the Fundamental Research Funds of Qilu Hospital of Shandong University (no. 26010175616016).

Acknowledgements

The authors thank Dr Xuewei Zhuang for excellent technical assistance.

References

Gao M, Chen L, Yang L, Yu X, Kou J & Yu B 2014 Berberine inhibits LPS-induced TF procoagulant activity and expression through NF-kappaB/p65, Akt and MAPK pathway in THP-1 cells. *Pharmacological Reports* **66** 480–484. (doi:10.1016/j.pharep.2013.12.004)

Guo T, Woo S, Guo X, Li H, Zheng J, Botchlett R, Liu M, Pei Y, Xu H, Cai Y, *et al*. 2016 Berberine ameliorates hepatic steatosis and suppresses liver and adipose tissue inflammation in mice with diet-induced obesity. *Scientific Reports* **6** 22612. (doi:10.1038/srep22612)

Han J, Liang H, Tian D, Du J, Wang Q, Xi P, Wang H & Li Y 2016 mTOR remains unchanged in diet-resistant (DR) rats despite impaired LKB1/AMPK cascade in adipose tissue. *Biochemical and Biophysical Research Communications* **476** 333–339. (doi:10.1016/j.bbrc.2016.05.123)

Jung T, Hong H, Hwang H, Yoo H, Baik S & Choi K 2015 C1q/TNF-Related Protein 9 (CTRP9) attenuates hepatic steatosis via the autophagy-mediated inhibition of endoplasmic reticulum stress. *Molecular and Cellular Endocrinology* **417** 131–140. (doi:10.1016/j.mce.2015.09.027)

Kim W, Lee Y, Cha S, Jeong H, Choe S, Lee M, Oh G, Park H, Lee K, Lane M, *et al*. 2009 Berberine improves lipid dysregulation in obesity by controlling central and peripheral AMPK activity. *American Journal of Physiology: Endocrinology and Metabolism* **296** E812–E819. (doi:10.1152/ajpendo.90710.2008)

Kim K, Jeong Y, Oh H, Kim S, Cho J, Kim Y, Kim S, Kim dH, Hur K, Kim H, *et al*. 2013 Autophagy deficiency leads to protection from obesity and insulin resistance by inducing Fgf21 as a mitokine. *Nature Medicine* **19** 83–92. (doi:10.1038/nm.3014)

Knebel B, Lehr S, Hartwig S, Haas J, Kaber G, Dicken H, Susanto F, Bohne L, Jacob S, Nitzgen U, *et al*. 2014 Phosphorylation of sterol regulatory element-binding protein (SREBP)-1c by p38 kinases, ERK and JNK influences lipid metabolism and the secretome of human liver cell line HepG2. *Archives Physiology Biochemistry* **120** 216–227. (doi:10.3109/13813455.2014.973418)

Lakshmipathi J, Alvarez-Perez JC, Rosselot C, Casinelli GP, Stamateris RE, Rausell-Palamos F, O'Donnell CP, Vasavada RC, Scott DK, Alonso LC, *et al*. 2016 PKCzeta is essential for pancreatic beta-cell replication during insulin resistance by regulating mTOR and cyclin-D2. *Diabetes* **65** 1283–1296. (doi:1210.2337/db1215-1398)

Lavallard V & Gual P 2014 Autophagy and non-alcoholic fatty liver disease. *BioMed Research International* **2014** 120179.

Le SV, Cinti A, Amorim R & Mouland A 2016 Adapting the stress response: viral subversion of the mtor signaling pathway. *Viruses* **8** 1528. (doi:10.3390/v8060152)

Levine B & Kroemer G 2008 Autophagy in the pathogenesis of disease. *Cell* **132** 27–42. (doi:10.1016/j.cell.2007.12.018)

Li X, Cen Y, Cai Y, Liu T, Liu H, Cao G, Liu D, Li B, Peng W, Zou J, *et al*. 2016 TLR9-ERK-mTOR signaling is critical for autophagic cell death induced by CpG oligodeoxynucleotide 107 combined with irradiation in glioma cells. *Scientific Reports* **6** 27104. (doi:10.1038/srep27104)

Liu LZ, Cheung SC, Lan LL, Ho SK, Xu HX, Chan JC & Tong PC 2010 Berberine modulates insulin signaling transduction in insulin-resistant cells. *Molecular and Cellular Endocrinology* **317** 148–153. (doi:10.1016/j.mce.2009.1012.1027)

Liu B, Jiang Y, Dong T, Zhao M, Wu J, Li L, Chu Y, She S, Zhao H, Hoffman RM, *et al*. 2016 Blockage of autophagy pathway enhances Salmonella tumor-targeting. *Oncotarget* **7** 22873–22882. (doi:22810.18632/oncotarget.28251)

Lu J, Cao Y, Cheng K, Xu B, Wang T, Yang Q, Yang Q, Feng X & Xia Q 2015 Berberine regulates neurite outgrowth through AMPK-dependent pathways by lowering energy status. *Experimental Cell Research* **334** 194–206. (doi:10.1016/j.yexcr.2015.04.006)

http://jme.endocrinology-journals.org
DOI: 10.1530/JME-16-0139

Published by Bioscientifica Ltd.

Ma D, Molusky M, Song J, Hu C, Fang F, Rui C, Mathew A, Pennathur S, Liu F, Cheng J, *et al*. 2013 Autophagy deficiency by hepatic FIP200 deletion uncouples steatosis from liver injury in NAFLD. *Molecular Endocrinology* **27** 1643–1654. (doi:10.1210/me.2013-1153)

Park K, Lee S, Kim T, Lee H, Lee C, Kim E, Jang J, Choi K, Kwon M & Kim Y 2007 A human scFv antibody against TRAIL receptor 2 induces autophagic cell death in both TRAIL-sensitive and TRAIL-resistant cancer cells. *Cancer Research* **67** 7327–7334. (doi:10.1158/0008-5472.CAN-06-4766)

Pyo J, Jang M, Kwon Y, Lee H, Jun J, Woo H, Cho D, Choi B, Lee H, Kim J, *et al*. 2005 Essential roles of Atg5 and FADD in autophagic cell death: dissection of autophagic cell death into vacuole formation and cell death. *Journal of Biological Chemistry* **280** 20722–20729. (doi:10.1074/jbc.M413934200)

Tiniakos D, Vos M & Brunt E 2010 Nonalcoholic fatty liver disease: pathology and pathogenesis. *Annual Review of Pathology* **5** 145–171. (doi:10.1146/annurev-pathol-121808-102132)

Wang N, Feng Y, Zhu M, Tsang C, Man K, Tong Y & Tsao S 2010 Berberine induces autophagic cell death and mitochondrial apoptosis in liver cancer cells: the cellular mechanism. *Journal of Cellular Biochemistry* **111** 1426–1436. (doi:10.1002/jcb.22869)

Wullschleger S, Loewith R & Hall M 2006 TOR signaling in growth and metabolism. *Cell* **124** 471–484. (doi:10.1016/j.cell.2006.01.016)

Xing L, Zhang L, Liu T, Hua Y, Zheng P & Ji G 2011 Berberine reducing insulin resistance by up-regulating IRS-2 mRNA expression in nonalcoholic fatty liver disease (NAFLD) rat liver. *European Journal of Pharmacology* **668** 467–471. (doi:10.1016/j.ejphar.2011.07.036)

Yan H, Xia M, Wang Y, Chang X, Yao X, Rao S, Zeng M, Tu Y, Feng R, Jia W, *et al*. 2015 Efficacy of berberine in patients with non-alcoholic fatty liver disease. *PLoS ONE* **10** e0134172. (doi:10.1371/journal.pone.0134172)

Zhang X, Zhao Y, Zhang M, Pang X, Xu J, Kang C, Li M, Zhang C, Zhang Z, Zhang Y, *et al*. 2012 Structural changes of gut microbiota during berberine-mediated prevention of obesity and insulin resistance in high-fat diet-fed rats. *PLoS ONE* **7** e42529. (doi:10.1371/journal.pone.0042529)

Zhang M, Zhou YF, Gong JY, Gao CB & Li SL 2016*a* Expression of autophagy-related protein LC3B, p62, and cytoplasmic p53 in human retinoblastoma tissues. *European Review for Medical and Pharmacological Sciences* **20** 3152–3160.

Zhang Q, Bian H, Guo L & Zhu H 2016*b* Pharmacologic preconditioning with berberine attenuating ischemia-induced apoptosis and promoting autophagy in neuron. *American Journal of Translational Research* **8** 1197–1207.

Zhang Z, Li B, Meng X, Yao S, Jin L, Yang J, Wang J, Zhang H, Zhang Z, Cai D, *et al*. 2016*c* Berberine prevents progression from hepatic steatosis to steatohepatitis and fibrosis by reducing endoplasmic reticulum stress. *Scientific Reports* **6** 20848. (doi:10.1038/srep20848)

Received in final form 2 September 2016
Accepted 21 September 2016
Accepted Preprint published online 21 September 2016

http://jme.endocrinology-journals.org
DOI: 10.1530/JME-16-0139

Published by Bioscientifica Ltd.